journal

J. Am. Ceram. Soc., 76 [10] 2695–700 (1993)

Tensile Creep and Creep-Strain Recovery Behavior of Silicon Carbide Fiber/Calcium Aluminosilicate Matrix Ceramic Composites

Xin Wu* and John W. Holmes*

Ceramic Composites Research Laboratory, Department of Mechanical Engineering and Applied Mechanics, The University of Michigan, Ann Arbor, Michigan 48109-2125

The tensile creep and creep strain recovery behavior of 0° and 0°/90° Nicalon-fiber/calcium aluminosilicate matrix composites was investigated at 1200°C in high-purity argon. For the 0° composite, the 100-h creep rate ranged from approximately $4.6 \times 10^{-9}\ s^{-1}$ at 60 MPa to $2.2 \times 10^{-8}\ s^{-1}$ at 200 MPa. At 60 MPa, the creep rate of the 0°/90° composite was approximately the same as that found for the 0° composite, even though the 0°/90° composite had only one-half the number of fibers in the loading direction. Upon unloading, the composites exhibited viscous strain recovery. For a loading history involving 100 h of creep at 60 MPa, followed by 100 h of recovery at 2 MPa, approximately 27% of the prior creep strain was recovered for the 0° composite and 49% for the 0°/90° composite. At low stresses (60 and 120 MPa), cavities formed in the matrix, but there was no significant fiber or matrix damage. For moderate stresses (200 MPa), periodic fiber rupture occurred. At high stresses (250 MPa), matrix fracture and rupture of the highly stressed bridging fibers limited the creep life to under 70 min.

I. Introduction

THE reinforcement of structural ceramics with whiskers and continuous fibers improves their toughness and reliability. Although the mechanisms of creep damage in whisker-reinforced ceramics have been extensively studied (an overview of the creep behavior of whisker-reinforced ceramics can be found in several papers by Wiederhorn and co-workers[1–3]), only a limited number of studies have addressed the creep behavior and mechanisms of creep damage in ceramic composites with continuous fiber reinforcement.[4–23] These investigations have shown that, in addition to the intrinsic creep behavior of the constituents, the transient redistribution in stress between the fibers and matrix plays a key role in the overall creep behavior and microstructural damage modes that occur during creep. To classify the creep damage modes in continuous-fiber-reinforced ceramics, Holmes and Chermant[22] have suggested the use of a creep rate mismatch ratio, defined as the ratio of the creep rate of the fibers to that of the matrix: CMR = $\dot{\varepsilon}_f/\dot{\varepsilon}_m$ (see discussions in Refs. 22 and 23). For composites with creep mismatch ratios less than unity, periodic fiber rupture can occur during long-duration tensile or flexural creep loading (this fiber rupture results from a redistribution in stress from the matrix to the more creep resistant fibers). This damage mode has been observed during the tensile creep of unidirectional SiC_f/HPSN composites.[18] For mismatch ratios greater than unity, matrix fracture has been identified as a characteristic creep damage mode for tensile and flexural loading histories (in this case a redistribution in stress from the fibers to the matrix occurs during creep loading). This latter damage mode was recently documented in SiC_f/RBSN composites subjected to tensile creep loading.[21]

The present investigation addresses the stress dependence of creep damage in a SiC-fiber-reinforced glass-ceramic composite and the influence of fiber layup on creep rate and creep-strain recovery. By conducting the experiments at a temperature close to the softening point of the matrix, it was possible to study creep damage accumulation for the limiting case of a creep mismatch ratio significantly less than unity.

II. Experimental Procedure

(1) Material and Specimens

Commercially available SiC-fiber/calcium aluminosilicate matrix composites (Nicalon SiC_f/CAS-II) were used in this study (processed by Corning Glass Works, Corning, NY). The composites, which contained 40 vol% Nicalon SiC fibers (Code NL-202, Nippon Carbon Co., Ltd., Yokohama, Japan), were hot-pressed as 0° panels with either 16 or 32 plies, and as 2D panels with a $[0/90]_{4S}$ ply layup (16 plies). To ensure that the creep behavior would not be influenced by intrinsic differences in the properties of the constituents, the fibers used in the panels were obtained from the same fiber spool. The specimens, shown in Fig. 1, had a gage length of 33 mm; the thickness was approximately 3.0 mm for the 16-ply panels and 6.0 mm for the 32-ply panels. To avoid damage to the fibers, the broad faces of

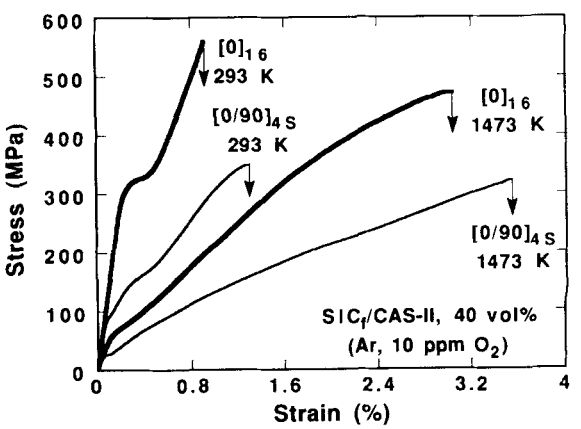

Fig. 1. Monotonic tensile behavior of $[0]_{16}$ and $[0/90]_{4S}$ Nicalon SiC_f/CAS-II composites at 20° and 1200°C. The experiments were conducted in high-purity argon (≤10 ppm O_2) at a loading rate of 100 MPa/s.

S. Wiederhorn—contributing editor

Manuscript No. 194497. Received June 4, 1993; approved July 12, 1993.
Presented in part at the 17th Annual Conference and Exposition on Composites and Advanced Ceramics, Cocoa Beach, FL, January 10–15, 1993 (Paper No. C-95-93F).
Supported by the National Science Foundation under Grant No. DMR-9257557.
*Member, American Ceramic Society.

Table I. Summary of Loading Histories and Experimental Results

Fiber layup	Loading history	ε_{100h} (%)	$\dot{\varepsilon}_{100h}$ (s^{-1})	$R_{cr,100h}$ (%)	$R_{t,100h}$ (%)
$[0]_{16}$	200 MPa/100 h	3.38	2.2×10^{-8}		
$[0]_{32}$	120 MPa/100 h	1.36	1.1×10^{-8}	23	32
$[0]_{32}$	60 MPa/100 h + 2 MPa/100 h	0.58	4.6×10^{-9}	27	33
$[0/90]_{4S}$	60 MPa/100 h + 2 MPa/100 h	0.59	4.0×10^{-9}	49	56
$[0/90]_{4S}$	60 MPa/100 h + 2 MPa/100 h	0.55	2.7×10^{-9}	45	52
$[0/90]_{4S}$	60 MPa/100 h + 2 MPa/100 h	0.62	3.9×10^{-9}	51	56
$[0/90]_{4S}$	60 MPa/40 min + 2 MPa/40 min			57/80*	73/70*

*Two 40-min cycles (first cycle/second cycle).

the specimens were not machined. The edges (minor faces) of the specimens were polished with diamond paste (down to 6 μm) to remove machining scratches and to prepare the surface for later microscopy.

(2) Load Frame, Grips, Extensometer

Tensile creep experiments were conducted on a servohydraulic load frame (Model 810, MTS Systems Corp., Minneapolis, MN) equipped with edge-loaded grips and an induction-heated SiC furnace. A mechanical extensometer with a gage length of 33 mm was used to measure gage-section strains. All experiments were conducted in high-purity argon. Using a residual gas analyzer (Delta F Corp., Model No. FA30111A, Woburn, MA), the partial pressure of oxygen in the chamber was consistently found to be between 5 and 10 ppm during the creep experiments (the slight variation in oxygen level was attributed to differences in the oxygen content of the argon cylinders that were used). The reader is referred to Ref. 24 for details concerning the grip and furnace designs, as well as information concerning the bending strains for the grip arrangement that was utilized.

(3) Outline of Creep Experiments

All creep experiments were conducted at 1200°C. At this temperature, the matrix will contribute little to the overall creep resistance of the composite (from the analysis of flexural creep data, Weber *et al.*[20] have estimated that approximately 95% of the creep load is carried by the fibers at 1200°C).

For the $[0]_{32}$ specimens, creep experiments were conducted at nominal stresses of 60, 120, 200, and 250 MPa (these stresses ranged from 13% to 52% of the monotonic strength at 1200°C). To obtain information regarding the strain recovery behavior of the composites, specimens that survived 100 h of creep were unloaded and held at a stress of 2 MPa for 100 h (the temperature was maintained at 1200°C). To determine if the creep behavior was influenced by the number of plies, a $[0]_{16}$ specimen was subjected to creep at 200 MPa. The influence of ply layup (0° versus 0°/90°) on creep behavior was examined by conducting creep experiments with 0°/90° specimens at a stress of 60 MPa. In addition, the effect of cycle duration on strain recovery behavior was examined by subjecting a 0°/90° specimen to 40 min of creep at 200 MPa followed by recovery for 40 min at 2 MPa (this test was stopped after two cycles). The loading histories used in the strain recovery experiments are summarized in Table I.

III. Results and Discussion

(1) Monotonic Tensile Behavior

The monotonic tensile behavior of the 0° and 0°/90° composites is shown in Fig. 1 for temperatures of 20° and 1200°C. At 1200°C, the 0° specimens exhibited a detectable deviation from linear behavior at a stress of approximately 70 MPa, with an ultimate strength of approximately 480 MPa.

(2) Tensile Creep Behavior and Stress Dependence of Creep Rate

Tensile creep curves (strain versus time) are shown in Fig. 2(a) for the 16- and 32-ply unidirectional specimens. Comparing the 200-MPa creep curves for the 16- and 32-ply specimens, the number of plies does not appear to significantly influence creep behavior. For creep stresses between 60 and 200 MPa, no failures of the 32-ply specimens were observed within the 100-h limit of the experiments. For this stress interval, the creep rate decreased continuously with time, with no apparent steady-state regime observed. Increasing the creep stress to 250 MPa resulted in creep rupture in roughly 70 min.

The stress dependence of tensile creep rate at 50 and 100 h is plotted in Fig. 2(b) for the 32-ply unidirectional specimens. The stress exponent for tensile creep was approximately 1.3 at both 50 and 100 h. These stress exponents are similar to that found for the creep of Nicalon fibers,[26] indicating that at 1200°C the creep rate of the composite was controlled by fiber creep.

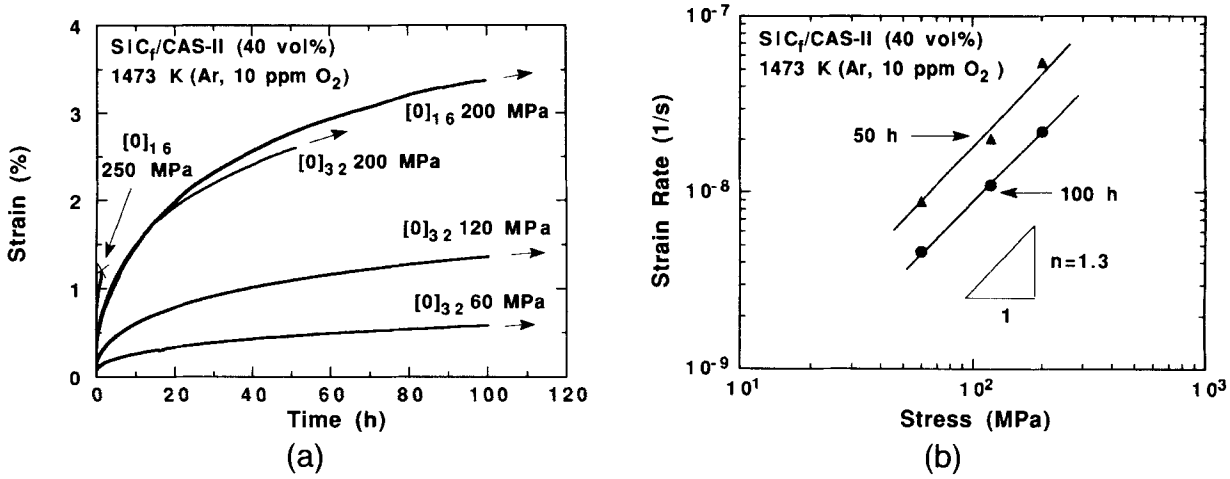

Fig. 2. (a) Total strain versus time for $[0]_{16}$- and $[0]_{32}$-Nicalon SiC$_f$/CAS-II composites crept at 1200°C in high-purity argon. (b) Stress dependence of 50- and 100-h creep rate for the unidirectional specimens. The experiment with the 32-ply specimen was stopped at 50 h to investigate creep damage accumulation.

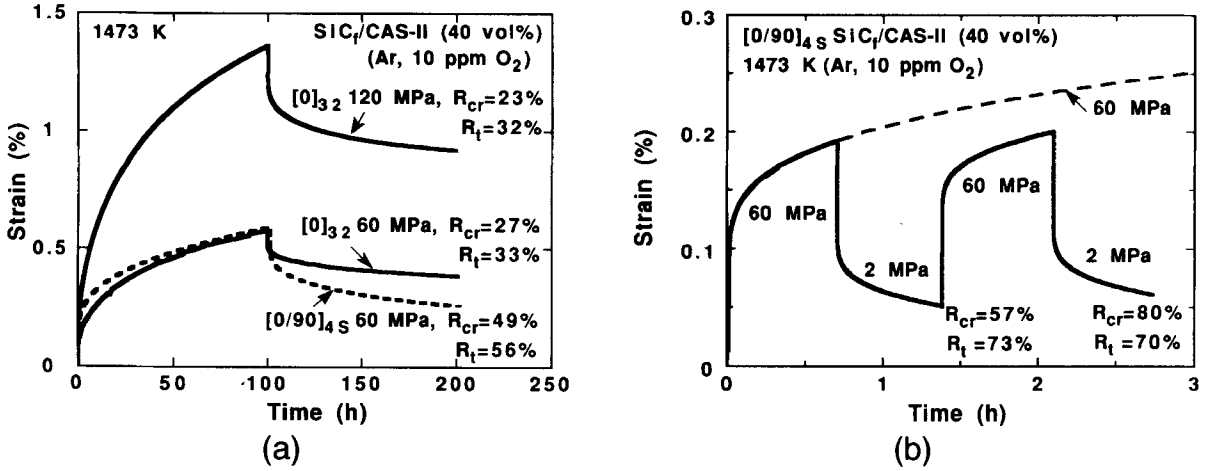

Fig. 3. Isothermal tensile creep and creep-strain recovery behavior of Nicalon SiC$_f$/CAS-II composites at 1200°C (the total strain is shown): (a) Cyclic creep behavior of $[0]_{32}$ and $[0/90]_{4S}$ composites. The creep rate of the $[0/90]_{4S}$ composite was similar to that of the unidirectional composite. (b) Short-duration cyclic creep behavior of $[0/90]_{4S}$ composites. The recovery creep strain is similar for both cycles; however, because of a reduction in transient creep, R_{cr} increased significantly for the second cycle.

(3) Creep-Strain Recovery

To quantify the amount of strain recovery that occurs during cyclic creep, it is convenient to define two recovery ratios:[18] the creep-strain recovery ratio, R_{cr}, and the total-strain recovery ratio, R_t. The creep-strain recovery ratio, R_{cr}, is defined as the creep strain recovered during a particular unloading cycle, $\varepsilon_{cr,R}$, divided by the creep strain for the cycle, ε_{cr}: $R_{cr} = \varepsilon_{cr,R}/\varepsilon_{cr}$. The total-strain recovery ratio, R_t, is defined as total strain recovered within a particular cycle ($\varepsilon_{el,R} + \varepsilon_{cr,R}$) divided by the total accumulated strain for the experiment, ε_t: $R_t = (\varepsilon_{el,R} + \varepsilon_{cr,R})/\varepsilon_t$.

Figure 3(a) shows the strain recovery behavior of 32-ply specimens that were crept at stresses of 60 and 120 MPa for 100 h and then unloaded to a stress of 2 MPa and held for 100 h. The creep-strain recovery ratio (R_{cr}) was 27% for creep at 60 MPa and 23% at 120 MPa (see Table I). Also shown in Fig. 3(b) is the recovery behavior of the 0°/90° composite after creep at 60 MPa. Interestingly, the 0°/90° composite showed essentially the same amount of strain accumulation and significantly more recovery than the 0° composite. As summarized in Table I, the creep-strain recovery ratio (R_{cr}) was 49% for the 0°/90° composite, compared to 27% for the 0° composite; the total-strain recovery ratios (R_t) were 56% and 33%, respectively. The higher recovery ratios for the 0°/90° composite were verified by two additional creep/recovery experiments conducted at 60 MPa. The creep-strain recovery ratios for these additional experiments were 45% and 51%; the total-strain recovery ratios were 52% and 56%. For the 0°/90° specimens, only one half of the fibers are in the axial loading direction; thus, intuitively, one would expect a much higher creep rate and strain accumulation for the same applied stress level. The similar strain accumulation, which was verified by duplicate testing, is attributed to the constraint to matrix creep provided by the rigid (noncreeping) fibers in the 90° orientation (this has also been verified by finite element analysis modeling of the creep behavior of 0°/90° composites—these results will be reported in a future paper by the authors). In effect, the transverse fibers increase the axial creep resistance of the matrix. The transverse fibers may also act to restrict movement of the axial fibers by direct contact. These results are considered very significant, since they clearly demonstrate the constraint to axial creep deformation provided by the transverse fibers.

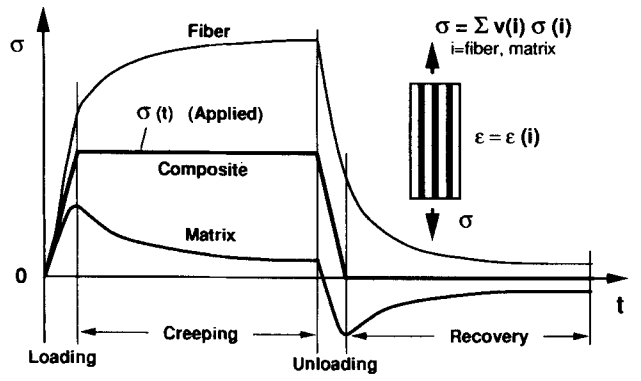

Fig. 4. Schematic representation of the redistribution in axial stress between the fibers and matrix during tensile creep and creep recovery. The curves assume that the fibers have a higher creep resistance and elastic modulus than the matrix. During creep the fiber stress progressively increases, while the matrix stress relaxes. Upon unloading, the stress in the fibers and matrix decreases. Note that the initial loading and unloading transients have been expanded for clarity. The actual stresses in the fibers and matrix during loading and unloading will depend upon the constitutive law and volume fraction of each constituent.

Figure 3(b) shows the recovery behavior of a 0°/90° specimen subjected to two cycles involving 40 min of creep at 60 MPa, followed by 40 min of recovery at 2 MPa. Compared to the 100 h creep/100 h recovery experiments described above, the strain recovery ratios were much higher for the shorter-duration creep cycles. For the first cycle, R_{cr} = 57% and R_t = 73%; for the second cycle these ratios were 80% and 70%, respectively (note that R_t decreases as the accumulated strain increases). A similar increase in the creep-strain recovery ratio for short-duration cyclic loading was also observed during cyclic creep experiments conducted with hot-pressed SCS-6 SiC$_f$/Si$_3$N$_4$ composites.[18] Careful inspection of Fig. 3(b) shows that the increase of the creep-strain recovery ratio on the second cycle was caused by a significant reduction in the duration of transient creep, which is attributed to a change in the residual stress state of the composite after the first loading/unloading cycle.

(4) Transient Creep and Creep-Strain Recovery Behavior: Redistribution of Internal Stresses

Numerical studies of the transient creep behavior of fiber-reinforced ceramics indicate that the initial transient creep behavior is to a large extent controlled by load transfer from the matrix to the fibers, which causes a time-dependent increase in elastic and creep strain (note that even in the absence of fiber creep, a time-dependent increase in elastic strain by load transfer would provide an overall increase in composite strain).[17]

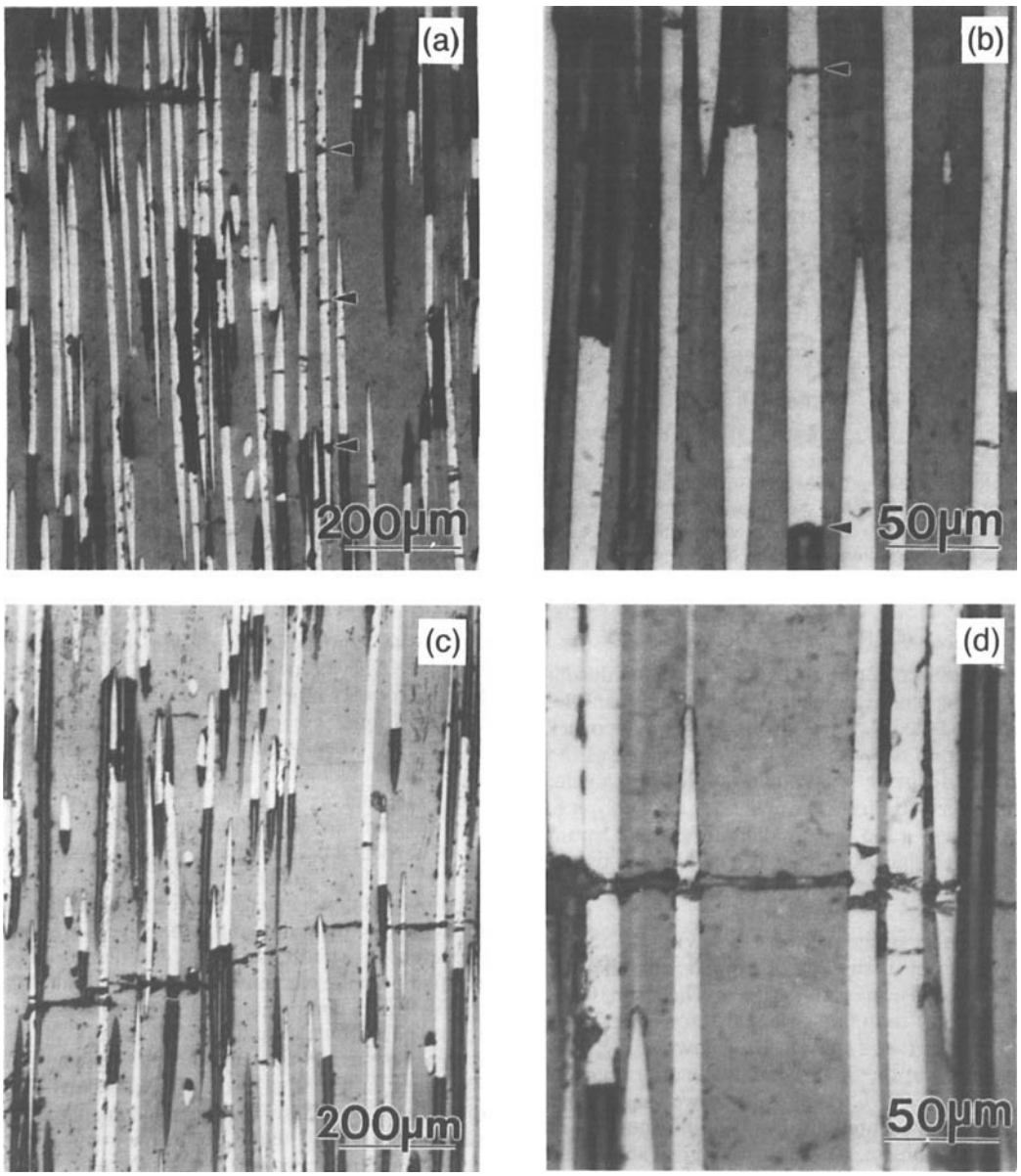

Fig. 5. Microstructural damage found after creep at 1200°C: (a,b) Periodic fiber fracture observed after 100 h at 200 MPa (the specimen did not fail). The arrows show the locations of periodic fiber fracture along one of the fibers. (c,d) Matrix fracture and rupture of bridging fibers observed after 70 min at 250 MPa (the micrographs were taken approximately 5 mm from the failure location of the specimen).

The concept of load transfer can be understood with reference to Fig. 4, which shows a schematic of the changes in axial stress in the fibers and matrix for a composite system where the matrix has a much lower creep resistance than the fibers. During application of a creep load, the fiber and matrix stress increase. After full application of the creep load, the matrix stress relaxes, and the fiber stress increases, as load is shed to the more creep-resistant fibers. The axial stress in the fibers progressively increases during creep, while the matrix stress decreases. Upon unloading, elastic contraction of the composite places the matrix in residual compression and the fibers in residual tension; with further time, creep-strain recovery results in relaxation of the tensile stress in the fibers and the compressive stress in the matrix. Overall, creep loading tends to increase the difference in stresses between the constituents, while creep-strain recovery tends to decrease differences in stress. In parallel with load transfer, there are several mechanisms that could give rise to the continually decreasing creep rate observed for creep stresses of 200 MPa and lower: (1) grain growth in the Nicalon fibers, which would lead to an *in situ* increase in creep resistance,[20] and (2) phase changes in the glass-ceramic matrix.

(5) Microstructural Investigation of Creep Damage

There were no observable fiber or matrix fractures in the specimen subjected to 100 h of creep at 60 MPa followed by 100 h of recovery; however, matrix cavities were found in the matrix. The cavities were generally located in fiber-rich regions of the microstructure. Similar cavity formation was observed by Weber *et al.*[20] during the 1200°C flexural creep of 0° Nicalon SiC_f/CAS composites. Increasing the creep stress to 120 MPa caused very limited matrix microcracking and fiber fracture; this damage is attributed to inhomogeneities in the fiber distribution, since the microcracking generally occurred in regions of the specimen that were matrix rich. At these low creep stresses, the matrix and fiber damage is stable, since both of these specimens exhibited a continually decreasing creep rate. The density and size of cavities had increased after creep at 120 MPa.

Both matrix cracking and periodic fiber rupture were found after 100 h of creep at 200 MPa (see Figs. 5(a) and (b)). Dissolving away the matrix using a molten (NaOH + KOH) solution at a temperature of about 500°C showed that the periodic fiber fracture occurred throughout the specimen. The matrix

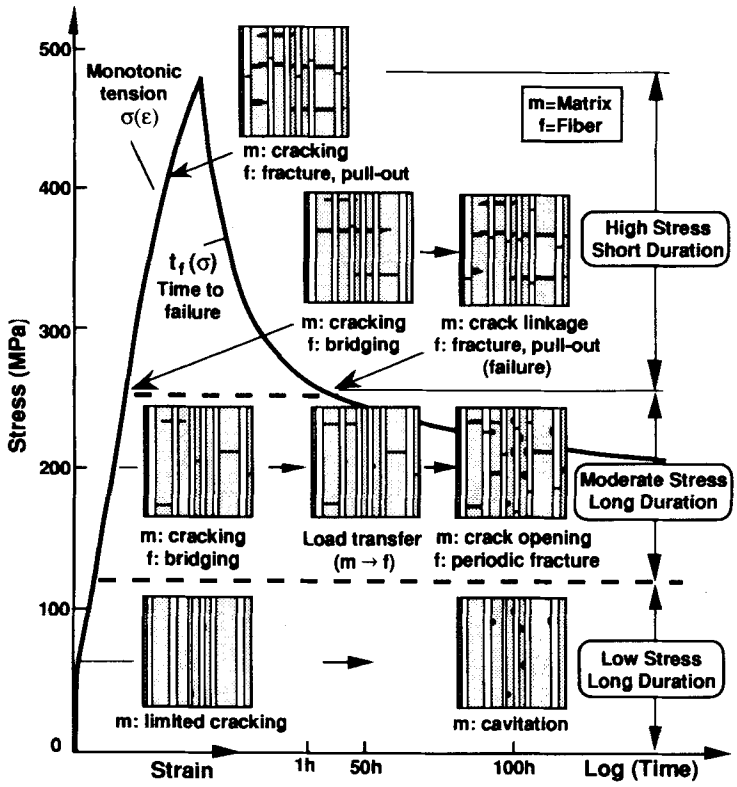

Fig. 6. Schematic diagram showing stress dependence of creep damage mode. At low stresses (<120 MPa) creep damage is limited to cavity formation in the matrix. At moderate stresses (120–200 MPa) periodic fiber fracture occurs. With higher creep stresses (≥250 MPa) failure occurs by rupture of the fibers that bridge matrix cracks.

cracks, which were located primarily in matrix-rich regions of the composite, were perpendicular to the tensile loading direction. These cracks appear to form during initial loading. However, because the matrix stress rapidly relaxes at the end of the loading transient, the cracks do not extend further during creep, but may open up parallel to the applied load as the bridging fibers undergo creep. The periodic fiber fracture can be explained by transient load transfer from the matrix to the more creep-resistant fibers, which causes an increase in fiber stress, and by time-dependent creep damage occurring in the fibers. Periodic fiber fracture, which has also been observed for the tensile creep of SCS-6 SiC/HPSN composites,[18] is a fundamental damage mode that occurs when the creep rate of the matrix significantly exceeds that of the fibers.

The creep life was less than 70 min at a stress of 250 MPa. At this stress level, significantly more matrix microcracking would occur during initial application of the creep load. Micrographs showing the matrix fracture and rupture of the bridging fibers found after creep at 250 MPa are shown in Figs. 5(c) and (d). Creep failure was most likely precipitated by fracture of highly stressed fibers that bridge initial matrix cracks; because the creep life was short, periodic fiber fracture remote from these initial cracks was not observed.

From the above discussion of creep damage, three different regimes can be identified for the 1200°C tensile creep of unidirectional Nicalon SiC_f/CAS-II composites: (1) low-stress/long-duration creep which leads to cavity formation, (2) moderate-stress/long-duration creep which is characterized by both cavity formation and periodic fiber fracture (without matrix fracture), and (3) high-stress/short-duration creep, characterized by the rupture of fibers that bridge matrix cracks. These regimes are illustrated schematically in Fig. 6. The damage modes described here are expected to hold for the tensile creep of other unidirectional composites where the matrix has a lower creep resistance than the fibers.

IV. Conclusions

The tensile creep and creep recovery behavior of 0° and 0°/90° Nicalon SiC_f/CAS-II composites was studied at 1200°C in high-purity argon. The following conclusions can be made regarding the creep behavior of this composite system:

(1) The 100-h creep rate of the 0° composite ranged from $4.6 \times 10^{-9}\ s^{-1}$ at 60 MPa to $2.2 \times 10^{-8}\ s^{-1}$ at 200 MPa. At 60 MPa, the 100-h creep rate of the 0°/90° composite was similar to that of the unidirectional composite, even though the 0°/90° had 50% fewer fibers in the loading direction. It was postulated that the transverse fibers improve the creep resistance of the matrix, and may also act to pin the 0° fibers.

(2) For the 0° composite, after 100 h of creep at 60 or 120 MPa, approximately 27% of the prior creep strain was recovered within 100 h of unloading. After 100 h of creep at 60 MPa, the creep-strain recovery ratio for the 0°/90° composite was significantly higher (45% to 51%) than that found for the unidirectional composites.

(3) Creep at 60 and 120 MPa for 100 h resulted in void formation in the matrix; only limited microstructural damage in the form of fiber and matrix fracture was found. After 100 h of creep at a moderate stress (200 MPa), periodic fiber fracture and void formation within the matrix were observed; only random matrix microcracking was found. The periodic fiber fracture, in the absence of matrix fracture, was attributed to the redistribution of stress from the matrix to the more creep resistant fibers.This creep damage mode is considered to be a fundamental damage mechanism in composites where the creep rate of the matrix significantly exceeds that of the fibers. At higher creep stresses (250 MPa), where the creep life was under 70 min, matrix fracture during initial loading causes high axial stresses in the fibers that bridge the matrix cracks, resulting in rupture of the bridging fibers and a correspondingly low creep life.

References

[1]B. J. Hockey, S. M. Wiederhorn, W. Liu, J. G. Baldoni, and S. T. Buljan, "Tensile Creep of Whisker-Reinforced Silicon Nitride," *J. Mater. Sci.*, **26,** 3931–39 (1991).

[2]S. M. Wiederhorn and B. J. Hockey, "High Temperature Degradation of Structural Composites"; presented at the 7th World Ceramics Congress (Montecatini Terme, Italy, June 24–30, 1990).

[3]S. M. Wiederhorn, "Creep and Creep Rupture of Ceramic-Matrix Composites"; pp. 239–64 in *Ceramics and Ceramic-Matrix Composites*, Vol. 3, Flight Vehicle Materials, Structures and Dynamics—Assessment and Future Directions. Edited by R. Levine. American Society of Mechanical Engineers, New York, 1992.

[4]J. J. Brennan and K. M. Prewo, "Silicon Carbide Reinforced Glass Ceramic Matrix Composites Exhibiting High Strength and Toughness," *J. Mater. Sci.*, **17,** 2371–83 (1982).

[5]K. M. Prewo, "Fatigue and Stress Rupture of Silicon Carbide Fibre-Reinforced Glass-Ceramics," *J. Mater. Sci.*, **22,** 2695–701 (1987).

[6]J. L. Chermant, "Research on Ceramic Matrix Composites in France," *Jpn. J. Appl. Phys., Part 2*, 179–86 (1989).

[7]F. Abbé, J. Vicens, and J. L. Chermant, "Creep Behavior and Microstructural Characterization of a Ceramic Matrix Composite," *J. Mater. Sci. Lett.*, **8,** 1026–28 (1989).

[8]F. Abbé and J. L. Chermant, "Creep Resistance of SiC–SiC Composites under Vacuum"; pp. 439–48 in Proceedings of the Fourth International Conference on Creep and Fracture of Engineering Materials and Structures. Edited by W. Wilshire and R. W. Evans. The Institute of Metals, London, U.K., 1990.

[9]F. Abbé and J. L. Chermant, "Deconvolution of Bending Creep Tests under Vacuum of 2D SiC-SiC," *J. Natl. Matér. Composites*, **7,** 401–10 (1990).

[10]F. Abbé and J. L. Chermant, "Fluage de Composites Céramiques," *Rev. Int. Hautes Temp. Refract.*, **27,** 103–17 (1991).

[11]D. Kervadec and J. L. Chermant, "First Results on the Creep Behavior of a SiC–MLAS Material"; in Proceedings of the Second European Ceramic Society Conference (Augsburg, Germany, September 11–14, 1991).

[12]D. Kervadec and J. L. Chermant, "Some Aspects of the Morphology and Creep Behavior of a Unidirectional SiC_f–MLAS Material"; pp. 459–71 in *Fracture Mechanics of Ceramics*, Vol. 10. Edited by R. T. Bradt *et al.* Plenum Press, New York, 1992.

[13]D. Kervadec and J. L. Chermant, "Behavior of 1D SiC_f-MLAS During Bending Creep Tests," *J. Natl. Matér. Composites*, **8,** 63–71 (1992).

[14]J. L. Chermant, F. Abbé, and D. Kervadec, "On the Creep Behavior of Long Ceramic Fiber Reinforced Ceramic Matrix"; pp. 371–90 in Proceedings of the 5th International Conference on Creep and Fracture of Engineered Materials and Structures. Edited by B. Wilshire and R. W. Evans. The Institute of Materials, London, U.K., 1993.

[15]J. W. Holmes, "Influence of Stress-Ratio on the Elevated Temperature Fatigue of a SiC Fiber-Reinforced Si_3N_4 Composite," *J. Am. Ceram. Soc.*, **74** [7] 1639–45 (1991).

[16]J. W. Holmes, "Tensile Creep Behavior of a Fiber-Reinforced SiC–Si_3N_4 Composite," *J. Mater. Sci.*, **26,** 1808–14 (1991).

[17]Y. Park and J. W. Holmes, "Finite Element Modeling of Creep Deformation in Fiber-Reinforced Ceramic Composites," *J. Mater. Sci.*, **27,** 6341–51 (1992).

[18]J. W. Holmes, Y. H. Park and J. W. Jones "Tensile Creep and Creep Recovery Behavior of a SiC-Fiber–Si_3N_4-Matrix Composite," *J. Am. Ceram. Soc.*, **76** [5] 1281–93 (1993).

[19]J. W. Holmes and J. Morris, "Elevated Temperature Creep of a 3-D C_f/SiC Composite"; presented at the 15th Annual Conference on Ceramics and Advanced Composites, Cocoa Beach, FL (January 1991).

[20]C. H. Weber, J. P. A. Lofvander and A. G. Evans, "The Creep Behavior of CAS/Nicalon Continuous-Fiber Composites," submitted to *Acta Metall.*

[21]G. E. Hilmas, J. W. Holmes, R. T. Bhatt, and J. A. DiCarlo, "Tensile Creep Behavior and Damage Accumulation in a SiC-Fiber/RBSN-Matrix Composite"; pp. 291–304 in Ceramic Transactions, Vol. 38, *Advances in Ceramic Matrix Composites*. Edited by N. Bansal. American Ceramic Society, Westerville, OH, 1993.

[22]J. W. Holmes and J.-L. Chermant, "Tensile Creep Behavior of Fiber-Reinforced Ceramic Matrix Composites"; to be published in the Proceedings of the HT-CMC Conference (ECCM-6), Bordeaux, France, September 1993.

[23]J. W. Holmes, "Elevated Temperature Deformation and Fatigue Deformation of Fiber Reinforced Ceramic Matrix Composites; in *Elevated Temperature Mechanical Behavior of Fiber-Reinforced Ceramics*. Edited by S. Nair and K. Jakus. Butterworth Hienneman, in press.

[24]J. W. Holmes, "A Technique for Tensile Fatigue and Creep Testing of Fiber-Reinforced Ceramics," *J. Compos. Mater.*, **26** {6} 916–33 (1992).

[25]R. Stewart, Corning Glass Works, Corning, NY; personal communication, December 1991.

[26]A. R. Bunsell, G. Simon, Y. Abe, and M. Akiyama; pp. 427–78 in *Fiber Reinforcements for Composite Materials*. Edited by A. R. Bunsell. Elsevier, Amsterdam, Netherlands, 1988. □